INTERNATIONAL STANDARD

ISO TC 20 / SC 14 / WG 4
ISO/WD 22009
WORKING DRAFT

Space System - Space Environment (Natural and Artificial)

Model of Earth's Magnetospheric Magnetic Field

(Explanatory Report, Revision 4)

I.I. Alexeev, V.V. Kalegaev, Yu.G. Lyutov, M.I. Panasyuk,
Skobeltsyn Institute of Nuclear Physics,
Moscow State University , Russia

J. M. Quinn,
Geomagnetics Group, U. S. Geological Servey MS 966
Federal Center, Denver, CO 80225-0046, U. S. A.

06 May, 2003

Explanatory Report

1 Background

The proposed ISO standard is a magnetic field model of the Earth's magnetosphere. It is intended to calculate the magnetic induction field generated from a variety of current systems located on the boundaries and within the boundaries of the Earth's magnetosphere under a wide range of environmental conditions, quiet and disturbed, affected by Solar-Terrestrial interactions simulated by Solar activity such as Solar Flares and related phenomena which induce terrestrial magnetic disturbances such as Magnetic Storms.

The current (fourth) revision of the Explanatory report is based on recommendation about the model users and their requirements which described in Resolution 145 of 16-th ISO TC20/SC14/WG4 Meeting at Houston, USA (October, 2002) as well as on "Report by IAGA Division V on a Survey of Magnetospheric Modellers Re-sponses to the Proposed ISO Standard" by Vladimir Papitashvili and Alan Thomsonas and on comments made by Tuija Pulkkinen (FMI).

1.1 Purposes and scope

The goals of standardization of the Earth's magnetospheric magnetic field are:

- providing the unambiguous presentation of the geomagnetic field of currents flowing inside the Earth and the magnetic field of magnetospheric currents;
- providing comparability of results of interpretation and analysis of space experiments;
- providing less labour-consuming character of calculations of the magnetic field of magnetospheric currents in the space at geocentric distances of 1-6.6 Earth's radii (R_E);
- providing the most reliable calculations of all elements of the geomagnetic field in the space environment.

The main purposes of elaboration of the "Model of the Earth's Magnetospheric Magnetic Field" Standard are

- standardization of method of presentation of the magnetospheric magnetic field as a sum of magnetic fields induced by large-scale magnetospheric current systems;
- standardization of the set of physical parameters of magnetospheric current systems ("key model parameters");
- standardization of the methods of magnetospheric magnetic field calculations by temporal variations of the magnetospheric current systems parameters;
- elaboration of the quantitative model of the Earth's Magnetospheric Magnetic Field dependent on physical parameters.

Technique of calculation of the main parameters of the magnetospheric model using data of measurements in the Earth's environment is not the subject of standardization.

The model elaborated in the framework of standard will work in

- Data Analyzing
- Watching the space environment conditions
- Forecasting the space environment conditions
- Warning the expected extremal conditions
- Postcasting and case study

1.2 Identification of users

The model will be useful for user communities working with space related applications in

- space weather forecasting;
- human health and insurance companies;
- radiation hazards determination;
- estimation of spacecraft and electronic devices integrity;
- pure and applied space physics environmental research;
- sattellite's navigation;
- satellite's communication;
- aero and space industry;
- fundamental scientists;
- students in space researches.

1.3 Users requirements

The ultimate objective of space weather research is the development of quantitative forecasting models. The main requirements of the Space Weather community to magnetospheric model are

- Model reliability:

    1. the model of the magnetospheric currents magnetic field must describe a regular part of the magnetic field, its dependence on the interplanetary medium parameters and reflects such magnetospheric magnetic field features as depression of the Earth's magnetosphere on the dayside due to its interaction with the solar wind, day and seasonal variations of the magnetic field;
    2. the model takes into account the tilt angle between the geomagnetic dipole and plane orthogonal to the Earth-Sun line varying within a range from -35 to +35 degrees;
    3. the model describes dynamics of the magnetospheric large-scale current systems;
    4. the model takes into account the dependence of the magnetic field of the magnetospheric current systems on the conditions in the Earth's environment;

5. the model enables taking into account variations of the magnetopause form and location as well as IMF penetration into the magnetosphere in dependence on solar wind conditions.

- Algorithm simplicity allowing the real-time (near real-time) calculations.
- The model must satisfy the well founded physical principles.
- The model is working without restrictions imposed on the values of interplanetary medium parameters that enable description of the disturbed and extremally disturbed magnetosphere for space weather forecastings.

1.4 Specification of the usefulness of the proposed standard

The model is used for instance to harden both spacecraft and the sensitive electronic devices carried by them from the effects of high-energy cosmic radiation. Space Weather Forecasting has value to the electrical utility community which can loose of millions of dollars in equipment such as transformers and in downtime due to magnetic storm induction effects at the Earth's surface. For example, during the March 1989 magnetic storm the Quebec Hydroelectric Utility grid failed costing on the order of 8600 million. Other utility grids around the world were also adversely affected by this storm. Transcontinental oil and gas pipelines are also susceptible to electromagnetic induction due to Space Weather, which causes corrosion and high-voltage hazards. Similar problems occur with spacecraft such as communications and weather satellites. These satellites are often in geostationary orbits. During a magnetic storm, the magnetospheric boundary, called the magnetopause, which ordinary acts as a deflecting shield against the Solar Wind is compressed inside the orbits of these satellites, leaving them exposed to the full impact of the Solar Wind's radiation. Sometimes the orientation of the satellites is determined by sensing the geomagnetic field. During a magnetic storm, when the magnetopause is compressed inside a satellite's orbit, the magnetic field orientation is suddenly reversed causing the satellite to abruptly rotate, which inturn causes extended booms (e.g. gravity gradient stabilization booms and others carrying electronic sensors) to snap off, leaving the satellite dysfunctional. The strong increase of the radiation belts ions as well as relativistic electron fluxes in the inner magnetosphere during magnetic storm main and recovery phases is the factor which can also be responsible for the geostationary satellite dysfunction and even losses. With sufficient warning through Space Weather forecasting, such damage can be minimized or eliminated.

Noting that over the past century the degree of Solar activity in terms of the number of sunspots occurring during the maximum of the 11-year Solar Cycle has generally been increasing from one cycle to the next, with some exceptions, and noting that the Earth's dipole magnetic field strength, which accounts for approximately 90% of the Earth's total magnetic field, is currently decreasing by approximately 7.14% per century, and further noting that Earth's dipole field strength has decreased by 50% in the past 2000 years, it is clear that the degree of penetration of energetic cosmic radiation to lower altitudes is correspondingly increasing. This in turn heats the upper atmosphere, which eventually affects the lower atmosphere and subsequently the daily weather and storm patterns at Earth's surface as well as posing human health hazards such as increased cancer risk due to increased radiation at the Earth's surface. The more energy penetrating into the Earth's atmosphere, the more active atmospheric weather patterns tend to be and the more severe are the solar related health hazards likely to be. These facts, plus our increased use of the space environment, mean substantially increased hazards related to Space

Weather over the next century. Knowledge through modeling of the magnetospheric environment and the resulting ability to predict its behavior are therefore becoming critical from the points of view of space mission accomplishment, health, economics, and natural disaster mitigation. Space Weather is clearly a global phenomenon, for which reason it is desirable to have an internationally accepted magnetospheric model.

1.5 Short review of relevant existing models

At present a lot of the models are used to calculate the magnetic field in the magnetosphere. The empirical models based on averaging of spacecraft experimental data (the OP-74, MF-73, T-87, T-89 models) allowing the real-time calculations and satisfactory describe the main magnetospheric magnetic field features during quite times but can not represent the magnetic field dynamics especially during disturbances. Their parameters are often non-physical and can not be changed according to rapidly changed magnetospheric conditions.

Versions of the Tsyganenko models, T96 [*Tsyganenko,* 1995], and T01 [*Tsyganenko,* 2002], use the observed values of $Dst, Bz_{\rm IMF}$, and the solar wind dynamic pressure to parameterize the intensity of the magnetospheric current systems. In the T96 model these parameters are replaced with the Kp index which has been used in the earlier versions of the Tsyganenko models. The T96 (as the earlier Tsyganenko models) was constructed using the minimization of the deviation from a data set of the magnetospheric magnetic field measurements gathered by several spacecraft during many years (the lage magnetospheric data base by *Fairfied,* [1994]. The disturbed periods are relatively rare events during the observation time, so their influence on the model coefficients is negligibly small. That is why the T96 model's applicability is limited by $Dst, Bz_{\rm IMF}$, and the solar wind dynamic pressure low values.

In T01 model the general approach remained the same as in the earlier T96 model, but the partial ring current with field-aligned closure currents was added. The new modeling database included 5-min average B-field data by the ISTP spacecraft Polar (1996-99) and Geotail (1994-99), as well as by earlier missions ISEE-2 (1984-87), AMPTE/CCE (1984-88), AMPTE/IRM (1984-86), CRRES (1990-91), and DE-1 (1984-90).

So-called dynamical models are based on mathematical equations derived from physical laws and allow calculations of magnetospheric magnetic field for any level of disturbance. The investigation of the magnetospheric current systems during magnetic storm is possible in terms of the modern dynamic models of the magnetospheric magnetic field (OP-88, HV-95, A96). An important advantage of the paraboloid model A96 [*Alexeev et al.,* 1996] is that it can describe the magnetic field of each magnetospheric current system as a function of its own time-dependent input parameters. A functional dependence of the model input parameters on the empirical data obtained by the satellites and on-ground observatories is determined by a set of submodels. The term "submodel" is used for the analytical definition of each model input parameter as a function of the empirical data.

The event-oriented models (see for example [*Ganushkina et al.,*, 2002]) are based on averaging of measurements data during one specific event and intended for the modeling of the processes during this event. Event-oriented modeling is needed for quite accurate representation of the observed magnetic field and can be very useful for validations of the existing global models. It allows to understand, how do they work for specific events, what could be improved in them?

2 Model Features

To satisfy to the projects purposes and to the users requirements the candidate model must include the following features:

1. day-side/night-side asymmetry (i.e., compression of the magnetosphere on the day-side and extension on the night-side due to the interaction of the Solar Wind with the internal geomagnetic field);
2. daily and seasonal variations;
3. the geomagnetic dipole inclination (tilt angle); relative to the plane orthogonal to the Earth-Sun line within a range of -35° to $+35^\circ$;
4. the close relation with the International Geomagnetic Reference Field (IGRF);
5. computation of the magnetospheric induction field includes:
   (a) the magnetic; field due to the Chapman-Ferraro currents on the magnetopause screening the dipole field;
   (b) the magnetic field due to the geotail current system magnetic field including the closure curren6ts on the magnetopause;
   (c) the magnetic field due to the ring current and partial ring current;
   (d) the magnetic field due to Region 1 and 2 field-aligned currents and closure ionospheric currents;
   (e) the magnetic field due to the magnetopause currents screening the ring current and other magnetospheric currents.
6. model depends on a small set of physical input parameters (model parameterization), characterizing the magnetospheric current sysytems intensity and location, such as geomagnetic dipole tilt angle, distance to the subsolar point of the magnetosphere as well as the other parameters, which can be different in the different models;
7. the input parameters depend on real-time, or near-real-time Empirical Data which can include solar wind and IMF data as well as Auroral Oval size and location, AL and Dst magnetic indices, long-term solar variability indices, sunspot number etc.;
8. the model characterizes the magnetospheric magnetic field under both quiet and disturbed conditions, without restrictions/limits imposed on the values of interplanetary medium or geomagnetic parameters and indices;
9. although in the framework of the proposed standard, the model is intended to be used inside the geostationary orbit it must be selfconsistently enable to provide calculations in the whole magnetosphere.

3 The Draft Model

The proposed ISO draft magnetic field model of the magnetosphere is intended to satisfy all of the requirements set forth in Section 2. Although this standard is intended to characterize the inner magnetosphere, the model must also merge smoothly into magnetic field generated in other regions of Earth's environment such as the core, the ionosphere, the distant tail, near-magnetopause regions and interplanetary space. Therefore, the International Geomagnetic Reference Field (IGRF) model, which describes the magnetic field generated by the Earth's core and which is produced by International Association of Geomagnetism and Aeronomy (IAGA) and updated by IAGA every 5 years is included as part of the proposed magnetospheric model. The total magnetic field is calculated as a sum of magnetic fields of internal (B_1) and magnetospheric (B_2) sources:

$$B_M = B_1 + B_2 \tag{1}$$

A model of the magnetic field generated by field-aligned currents, which connect the magnetosphere to the ionosphere, is also included as part of the magnetospheric model, as is a model of the magnetosheath magnetic field which takes into account the Interplanetary Magnetic Field (IMF) penetration into the magnetosphere. The model further includes a set of auxiliary physical models that characterize the magnetic field associated with various current systems on the magnetopause and within the magnetosphere itself. These include a model for the fields generated by Chapman-Ferraro currents on the magnetopause that screen the primarily dipole field of the Earth characterized by the IGRF model, a model characterizing fields generated by the geomagnetic tail current system, a model characterizing fields generated by the ring current system, and a model characterizing fields generated by those magnetopause currents that screen the ring current. The overall model is referred to as the Paraboloid Model A99 (Alexeev 99, described most completely in [*Alexeev et al.*, 1996; *Alexeev and Feldstein*, 2001]). In A99 magnetospheric magnetic field induction B_m is represented in the form:

$$B_2 = B_{sd}(\psi, R_1) + B_t(\psi, R_1, R_2, \Phi_\infty) + B_r(\psi, b_R) + B_{sr}(\psi, R_1, b_R) + B_{fac}(I_{||})$$

where

- B_{sd} is the magnetic field of Chapman-Ferraro currents on the magnetopause screening the dipole field;
- B_t is the geotail current system magnetic field;
- B_r is the ring current magnetic field;
- B_{sr} is the magnetic field of the magnetopause currents screening the ring current;
- B_{fac} is the field of Region 1 field-aligned currents.

The different magnetospheric magnetic field sources depend on different input parameters (model parametrization). The full set of the paraboloid model input parameters includes:

- ψ - geomagnetic dipole tilt angle
- $\mathbf{R_1}$ - distance to the subsolar point of the magnetosphere

- $\mathbf{R_2}$ - distance to the inner edge of the geotail current sheet
- $\mathbf{\Phi_\infty}$ - the tail lobe magnetic flux
- $\mathbf{I_{||}}$ - the total strength of Region 1 field-aligned currents
- $\mathbf{b_r}$ - the ring current magnetic field at the Earth's center

.

All the input parameters depend on empirical data from Solar Wind (which can be taken from the upstream solar wind monitors, today the ACE or Wind satellites), Auroral Oval data, and the AL and Dst magnetic indices computed from various geomagnetic observatories scattered around the Earth's surface. So, the model magnetic field sources depend on empirical data via input parameters. The different Submodels may be used to calculate the input parameters. The model user can choose his own Submodel which describe some input parameter dynamics based on his own data set. Thus, the paraboloid Model consists of three basic elements: Empirical data, Input Parameters, and the Model itself.

It should be noted that the submodels are not assumed to be standardization objects since they are created on the base of physical models. They are subject of the scientific investigations and can be changed in terms of the calculation techniques presented in Working Draft. It is possible to use the different models to calculate the input parameters. For example the empirical models of [*Roelof, Sibeck*, JGR, 1993, 98, 21421; *Shue et al.*, JGR, 1997, 102, 9497; *Kalegaev, Lyutov*, 2000, Adv. Space Res., 25, 1489] can be used for R_1 calculations via solar wind dynamic pressure and IMF B_z value. Three-level structure of the model, "experimental data – the parameters of the magnetospheric current systems – magnetospheric field", allows to user to use the different submodels to provide calculations for the case when the dataset is incomplete. Such approach allows flexible satisfy the user requirements involving them in the development of the model appropriated for their own needs and containing their own "physics".

Model is dynamic in the sense that it can function in real-time or near real-time depending on the availability of the empirical data. As was shown in the numerous papers (see Sec.4) and as presented in Appendix model functions through the full range of geomagnetic activity, from Solar Quiet conditions to severe magnetic storm conditions, and in the whole magnetosphere. Other magnetospheric models are commonly limited in their range of applicability with respect to geomagnetic activity and/or by the region of applicability in space.

3.1 Demonstration of model

Demonstration of model and methods' needs and opportunities for model development are presented in Appendix.

3.2 The model availability

The model is available at WWW site http://alpha.sinp.msu.ru/lvm/dynamod.html.

4 The Recent Project Activities

- Comparisons of the model calculations with the Large Magnetosphere Magnetic Field Data Base (Faierfield, Tsyganenko, et al., Journal of Geophysical Research, V.11, p.11319-11326, 1994) were made (see Appendix, Sec. 1).

- Detailed comparisons of the model calculations with observations in the course of several magnetic storms were made in the recently published papers:

  - V.V. Kalegaev, I.I. Alexeev, Y.I. Feldstein, L.I. Gromova, A. Grafe, M. Greenspan, (in Russian), *Geomagn. Aeronom., V. 38*, N 3, 10, 1998.
  - Dremukhina, L. A., Ya. I. Feldstein, I. I. Alexeev, V. V. Kalegaev and M. Greenspan, *J. Geophys. Res.*, *104*, N12, 28,351, 1999.
  - V.V.Kalegaev, and A. Dmitriev, *Advances in Space Research. 26*, N1, 117, 2000.
  - Alexeev, I. I., and Y. I. Feldstein, *J. Atmos. Sol. Terr. Phys., 63/5*, 331, 2001.
  - Kalegaev, V. V., I.I.Alexeev, Ya.I.Feldstein, *J. Atmos. Sol. Terr. Phys., 63/5*, 473, 2001.
  - Alexeev I.I., E.S.Belenkaya, R. Clauer, *Journ. of Geoph. Res., 105*, 21,119, 2000.
  - R. Clauer, Alexeev I.I., E.S.Belenkaya, *Journ. of Geoph. Res., 106*, 25695, 2001.
  - Alexeev, I. I., V. V. Kalegaev, E. S. Belenkaya, S. Y. Bobrovnikov, Ya. I. Feldstein and L. I. Gromova, *Journ. of Geoph. Res., 106*, 25683, 2001.
  - Feldstein, Y.I., L.A. Dremukhina, A.E. Levitin, U. Mall, I.I. Alexeev, and V.V. Kalegaev, Energetics of the magnetosphere during the magnetic storm, Journ. of Atm. and Sol.-Terr. Phys., V.65, No.4, pp 429-446, 2003.

  (see also Appendix, Sec.2).

- The Authors' Version and Working Draft of Project have been sent to interested scientists and specialists to 11 countries. The Authors' Version and Working Draft of Project have been reviewed and corrected by the scientists and specialists from

  - **France:** Daniel M. Boscher (ONERA-CERT/DESP)
  - **Japan:** Hiroshi Suzuki, Yukihito Kitazawa (Ishikawajima-Harima Heavy Industries Co., Ltd.), Prof. T. Iemori (Kyoto University)
  - **Russia:** Dr. Alexandr Schevurev (STC "Kosmos") and Dr. V.P. Nikitskiy (RS Corp. "Energiya")
  - **Finland:** Tuija Pulkkinen, Natasha Ganushkina (Finnish Meteorological Institute)

- The magnetic field of the Region 1 field aligned current system is included in the draft model.

- The Web site of the Project has been created (http://alpha.sinp.msu.ru/iso/)

- The project "SPACE ENVIRONMENT (NATURAL AND ARTIFICIAL). MODEL OF THE EARTH'S MAGNETOSPHERIC MAGNETIC FIELD." has been discussed and approved at the recent Meetings of WG4.

  - In accordance with resolution, taken at the plenary meeting of TC20/SC14/WG4 in Brazil, and with request made by James E. French (Secretary of ISO TC20/SC14), the Approved Work Item (AWI) "Space systems - Space environment - Model of the Earth's magnetospheric magnetic field" has been registered with the ISO Central Secretariat and given the number 22009.
  - In accordance with resolution 122, taken at the plenary meeting of TC20/SC14/WG4 in Tolouse (October, 2001) the current draft standard was examined and revised to incorporate new content and format as described in resolution 114 of the Meeting.
  - At the plenary meeting of TC20/SC14/WG4 in Noordwijk, Netherlands (May, 2002) the experts of WG4 confirm the necessity of involving th IAGA experts in the comparative analysis of existing magnetic field models.
  - In accordance with resolution 145 approved by 16-th ISO TC20/SC14/WG4 Meeting at Houston, USA (October, 2002) WD22009 was reexamined and revised to incorporate new recommendation about the model users and their requirements obtained from IAGA representatives

- The new comparison of the model calculations with experimental data as well as the models cross-comparisons was made. The results of comparison are published in the international journals (more 20 refereed articles from 1998).

5 Contacts with IAGA WG3

In response to the request from the ISO/TC20/SC14/WG4 committee on the 'Space Environment (Natural and Artificial)' the Division V and Working Group 3 of International Association for Geomagnetism and Aeronomy (IAGA) carried out an assessment of the need for and relevance of a 'standard magnetospheric model' within the community of magnetospheric scientists. Based on the 5 responses of modellers, a negative, in general, attitude toward the magnetospheric magnetic field standard elaboration was done.

The main reason against the magnetospheric field standard elaboration was connected with this proposition that it will restrict the future development of magnetospheric models and does not give the possibility to create any alternative models. The main recommendation from IAGA representatives is to reconsider the current ISO approach to magnetospheric field model standardization. It was recommended to establish a framework, that is, a documented list of requirements, allowing ISO certification of various existing models, including the current candidate model as a working example. Although such an approach makes it more difficult to further develop the project, and changes the work plans, the MSU working group is ready to discuss it within ISO standard procedure involving the IAGA Division V and Working Group 3 representatives and based on the new and previously obtained reports from the experts. MSU working group agrees with the comments regarding the new model checking on the real data and ready to present paraboloid model for the independent testing and cross comparing with the other candidate models (if any). However, this activity must be carried out within the existing already Project timetable accepted and approved by ISO TC20/SC14/WG4 and without the destroying the existing ISO procedure of the Standard development.

6 The Preliminary Work Plan

- Improvement of the existing models of the magnetic field sources.
- Define more precisely the model input parameters and techniques of their determination from measurement data.
- Work out the interfaces of programs which would enable utilization of the resources of space physics data bases.
- Elaborate a family of models which allow calculations of the magnetic field in the magnetosphere, in the case of lacking measurement data for several of necessary model parameters (with somewhat decreased accuracy).
- Estimate an accuracy of the model and compare the latter with other available models.
- Continue the evaluation and cross-comparison with the models available as well as model testing, verification and code validation.

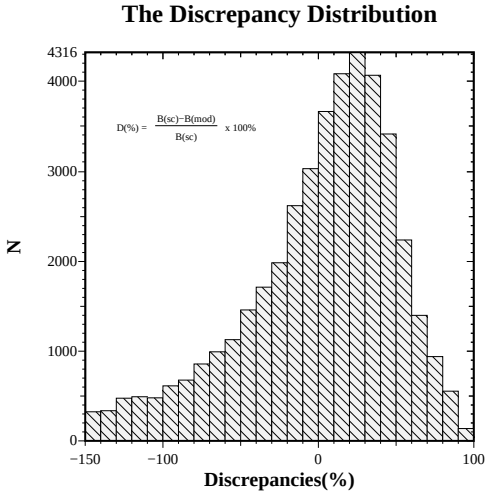

Figure 1: The distribution of discrepancies of magnetospheric field magnetic induction calculated in term of the parabolic model, compared with experimental data. $B(sc)$,nT, is the field measured onboard spacecrafts, $B(mod)$,nT, is the field calculated in terms of the parabolic model, N is for statistics.

APPENDIX. Accuracy of the Model and Comparison With Experimental Data

In this section we show the examples of paraboloid model usage and comparison with the other models. There are the comparison with the Large Magnetosphere Magnetic Field Data Base (subsection A1), calculation of the magnetic field during January 1997 magnetic storm, calculation of the magnetic field during September 1998 magnetic storm using the advanced submodels and the cross-comparison of the paraboloid model, T01 model and event-oriented model by [*Ganushkina et al.*, 2002, 2003] for the 25-26 June 1998 case study.

A1. Stationary Case. Comparison with the Large Magnetosphere Magnetic Field Data Base

The comparison with the Large Magnetosphere Magnetic Field Data Base (Faierfield et al., Journal of Geophysical Research, V.99, p.11319-11326, 1994) was made. Data base includes data of Explorer 33,35, IMPs 4,5,6,7,8, Heos 1,2 and ISEE 1, 2 in the region between 4 and 60 R_E. Calculations of the input parameters of the model were performed using solar wind data, D_{st} and AL indices which are contained in Data Base. Parameters ψ, R_1, Φ_∞ were calculated in terms of submodels presented in Appendix 1 of Working Draft. Field-aligned currents magnetic field was not taken into account in these calculations as the first step of the model evaluation.

It was supposed

$$R_2 = 1/\cos^2\varphi_k \qquad D_{st} < -10nT$$
$$R_2 = 0.7R_1 \qquad D_{st} > -10nT$$
$$b_r = D_{st} \qquad D_{st} < -10nT$$
$$b_r = -10nT \qquad D_{st} > -10nT,$$

where φ_k is the midnight latitude of the equatorward boundary of the auroral oval.

Fig.1 and 2 represent this comparison in the form of the distribution of discrepancies. The histogram in Fig.1 shows the distribution of relative discrepancies $D = \frac{B(sc)-B(mod)}{B(sc)} \cdot 100\%$ integral over the whole experimental material (45181 measurements). The discrepancy mean value is about +3% (the distribution is asymmetric with a long negative "tail"), σ of the distribution

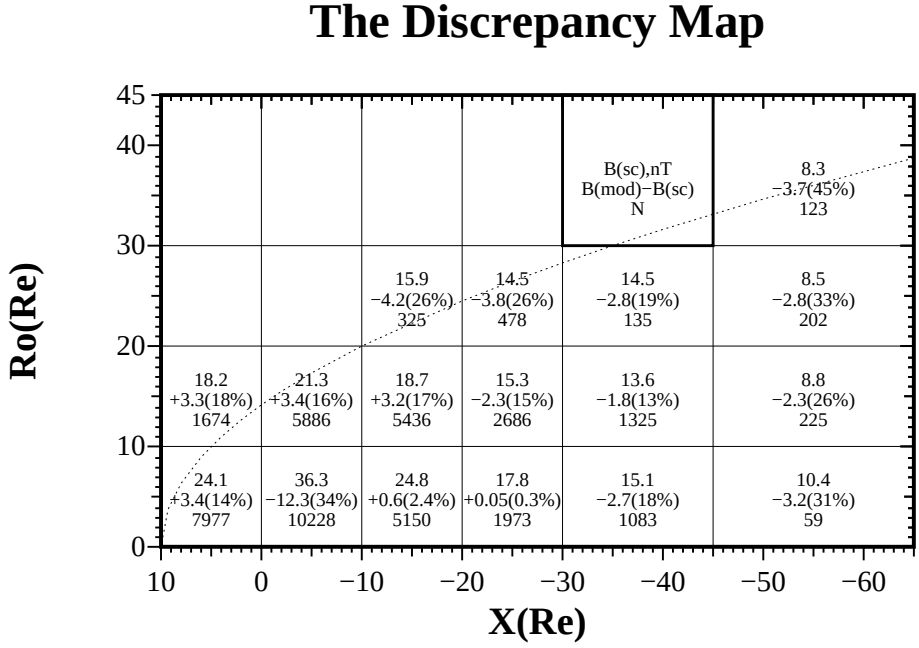

Figure 2: The distribution of the discrepancies of magnetospheric magnetic field calculated in term of the paraboloid model A99, compared with experimental data. In the singled out cell the format of data is shown: $B(sc)$,nT, is the measured onboard spacecrafts magnetic field averaged in cells, $B(mod)$,nT, is the average field calculated in terms of the paraboloid model, N is for statistics.

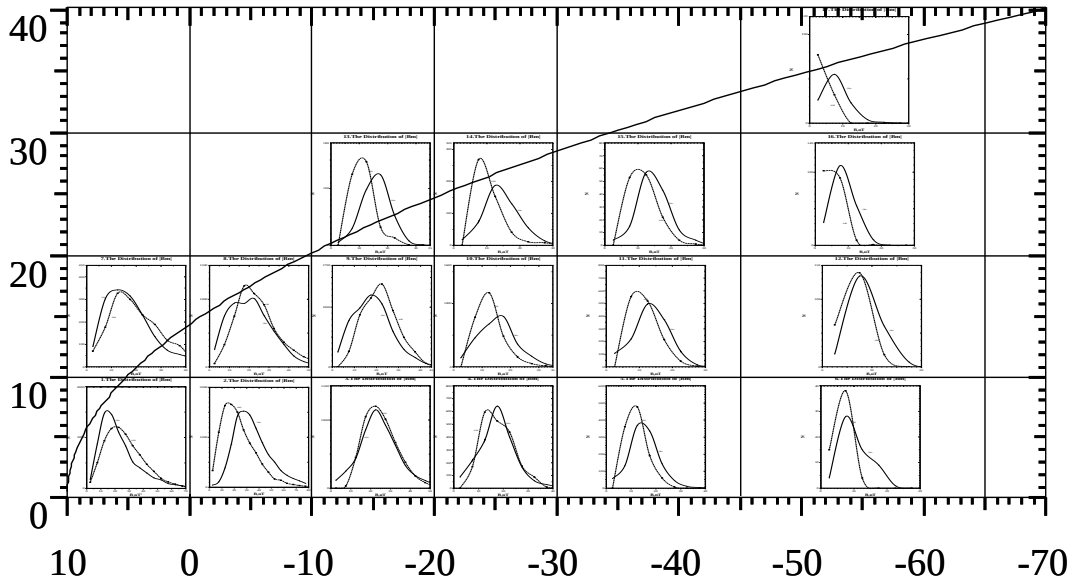

Figure 3: The magnetic field module distributions in the different cells of the magnetosphere, measured (solid line) and calculated by paraboloid model A99 (thin line).

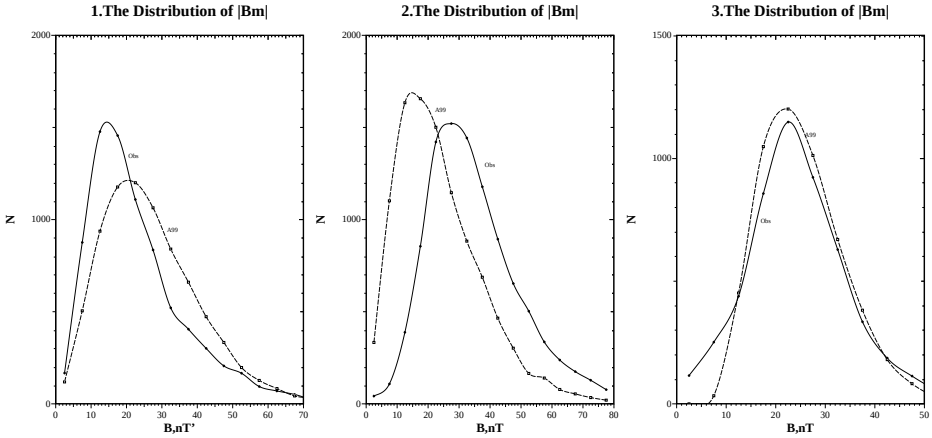

Figure 4: The magnetic field module distributions (measured and calculated by A99) in the near-Earth (x, ρ) cells (10:0; 0:10), (0:-10; 0:10), (-10:-20; 0:10) of the magnetosphere.

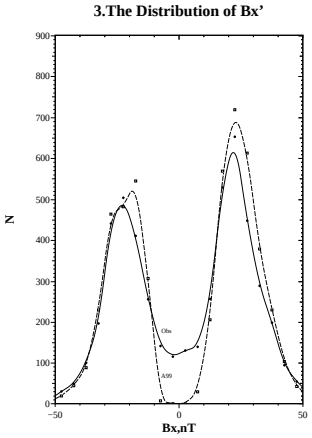

Figure 5: The same as in the Fig. 4 for GSM Bx component of the magnetospheric magnetic field.

being of $\sim 80\%$. Fig. 2 presents the distribution of absolute and relative discrepancies differential in x and ρ, where $\rho = \sqrt{y^2 + z^2}$, x, y, z are the solar-magnetospheric (GSM) coordinates. The weight of each discrepancy value (statistics) is shown in the corresponding cell in x and ρ. An examination of the Fig.2 shows that near the Earth at distances about the geostationary orbit in the magnetosphere nightside the discrepancy is, on average, 12.3 nT for $-10 < x \leq 0$ and $0 \leq \rho < 10$, and in the magnetosphere dayside it is, on average, 3.4 nT for $0 < x \leq 10$ and $0 \leq \rho < 10$.

The magnetic field module distributions in the different cells of the magnetosphere, measured and calculated by paraboloid model are represented in the Figure 3. The measured magnetic field has also an own non-Gaussian distribution in each cell. The mean values and discrepancies represented in the Fig. 2 are the measured magnetic field distribution mean values and mean discrepancies between measured and calculated values. The calculated by paraboloid model magnetic field is distributed in a good agreement with observations.

Fig.4 represents the distributions in (x, ρ) cells (10:0; 0:10), (0:-10; 0:10), (-10:-20; 0:10) respectively. The first and second cells demonstrate the regular shifts: the magnetic field in the night side is underestimated and in the dayside is overestimated. Such behavior can be explained by field aligned currents effect which is not taken into account in these calculations.

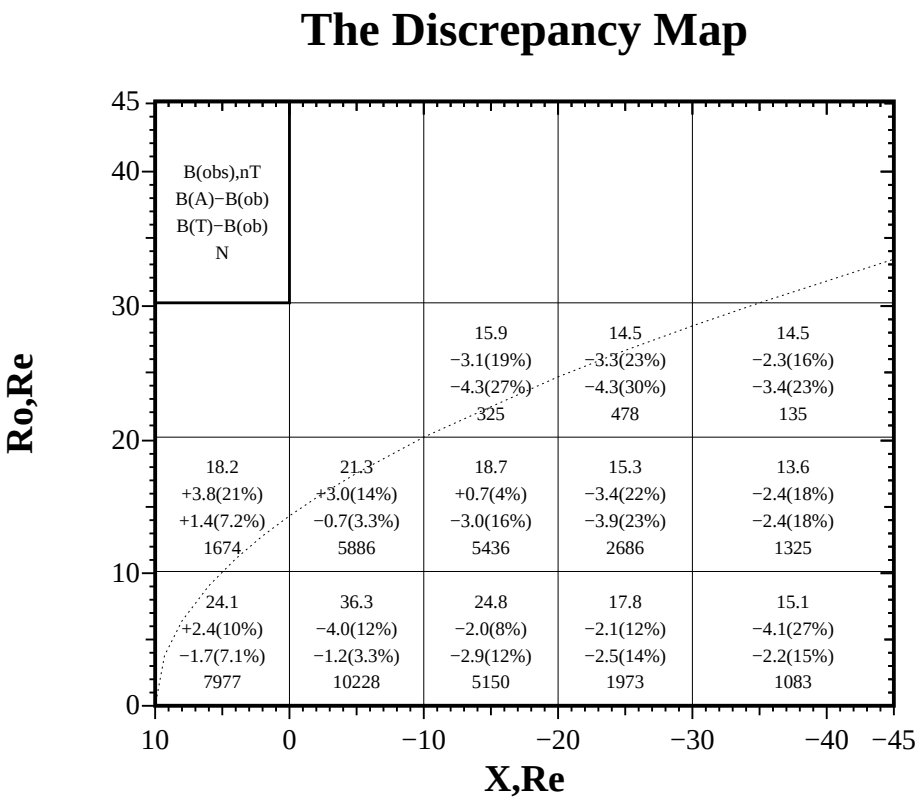

Figure 6: The same as in the Fig. 3, calculated in terms of A01 and T96 models

The quite good agreement exists in the third cell.

Fig. 5 represents the same comparison for the GSM Bx component of the magnetic field in the (x, ρ) cell (-10:-20; 0:10). The distribution depression near the $Bx = 0$ corresponds the measurements which were made in the tail plasma sheet region. The A99 paraboloid model has infinite thin tail current so the Bx values which are about of zero are absent.

Paraboloid model allows flexible taking into account the new magnetospheric magnetic field sources. Moreover, because each magnetospheric magnetic field source with its own screening currents is calculated separately and depends linearly on its own input parameters we can change the parametrization of current systems to match better the data. To take into account the mentioned above effects of field aligned currents and "thin" tail current the new "beta" version of paraboloid model (A01) was developed. The "thin geotail" magnetic field [*Alexeev and Bobrovnikov, 1997*] and field aligned current magnetic field [*Alexeev, Belenkaya and Clauer, 2001*] were taken into account. Fig. 6 shows the measured magnetic field module mean values in the different cells of the magnetosphere as well as mean discrepancies between the measured magnetic field and calculated by A01 (second row) and T96 (third row). The more good agreement for A01 is detected in the near-Earth region than that represented in the Figure 2. We can see that in general, the obtained in terms of A01/A99 discrepancies are of the same order as those obtained in the framework of T96 model [*Tsyganenko*, 1995].

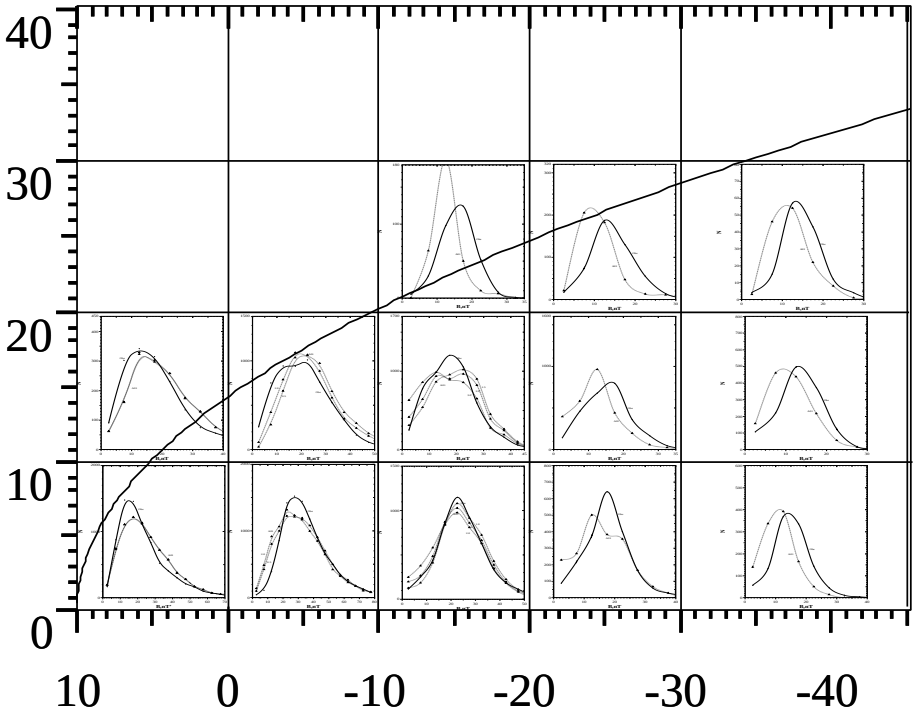

Figure 7: The magnetic field module distributions over the whole statistics in the different cells in the Earth's magnetosphere, measured and calculated by A01 model.

The magnetic field module distributions in the different cells of the magnetosphere, measured and calculated by paraboloid model are represented in the Figure 7. The magnetic field distributions measured in the near-Earth's cells represented in the Figures 8 (magnetic field module) and 9 (Bx component). The distributions of the magnetic field calculated for the different parameterizations of the tail current and field aligned currents demonstrate the more good agreement with experimental data of calculations obtained in the framework of A01 paraboloid model than that obtained by A99 model.

The results represented on the Fig. 6 shows that paraboloid model, analytical and based on the small number of the input parameters, describes the large array of experimental data with approximately the same accuracy as the T96 model, which constructed as approximation of that array. Fig. 10 represents the distributions of measured and calculated by A99 and T96 models

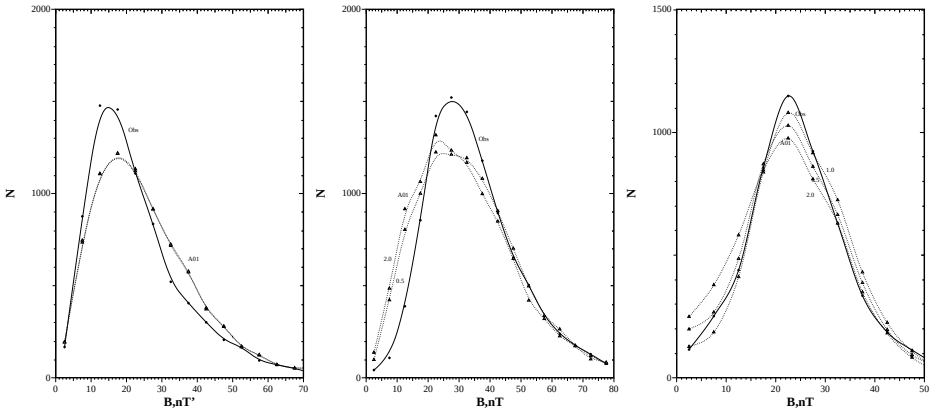

Figure 8: The same as in the fig. 4 for magnetic field module calculated by A01 model.

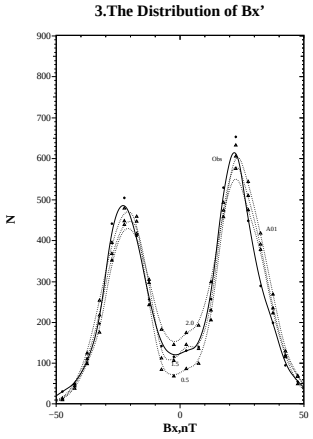

Figure 9: The same as in the fig. 8 for Bx component of the magnetospheric magnetic field.

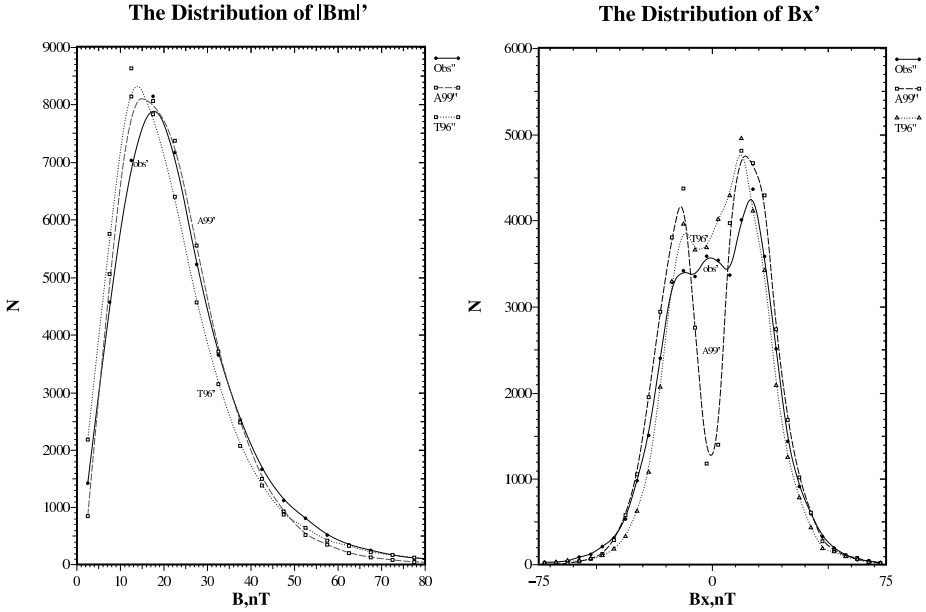

Figure 10: The same as in the fig. 8 for Bx component of the magnetospheric magnetic field.

magnetic fields (module and Bx component, respectively).

In the Table 1 the comparison of magnetic field calculated by paraboloid model (A99) Tsyganenko model (T96) and measured magnetic field from Large Magnetosphere Magnetic Field Data Base averaged by the levels of disturbances is presented. We can see that only for very quite conditions T96 model gives the better results than A99. For Kp between 1^- and 2^- the results are comparable, but for disturbed conditions ($Kp > 2$) A99 gives the better results than T96. The T96 (as the earlier Tsyganenko models) was constructed using the minimization of the deviation from a data set of the magnetospheric magnetic field measurements gathered by several spacecrafts during many years. The disturbed periods are relatively rare events during the observation time, so their influence on the model coefficients is negligibly small. That is why the T96 model's applicability is limited by $Dst, Bz_{\rm IMF}$, and the solar wind dynamic pressure low values.

Kp	A99	T96	Data
$0, 0^+$	13.8	**14.9**	15.5
$1^-, 1$	**16.9**	16.3	17.6
$1^+, 2^-$	18.3	**18.6**	20.3
$2, 2^+$	**21.6**	20.6	22.6
$3^-, 3, 3^+$	**25.3**	24.1	26.3
$4^-, 4, 4^+$	**30.0**	28.1	31.3
$5^-, 5$	**34.8**	33.4	35.4

Table 1: Comparison of magnetic field calculated by paraboloid model (A99) Tsyganenko model (T96) and measured magnetic field from Large Magnetosphere Magnetic Field Data Base averaged by the levels of disturbances.

A2. Nonstationary Case. Case study for January 9–12, 1997

The dynamics of the magnetospheric current systems was studied in [*Alexeev et al.*, 2001] in terms of A99 model for the specific magnetospheric disturbance on January 9–12, 1997 caused by the interaction of the Earth's magnetosphere with a dense solar wind plasma cloud. A dense cloud of the solar wind plasma was of rather complicated structure. A southward interplanetary magnetic field (IMF) in its leading part caused a significant substorm activity during the interaction with the magnetosphere. A strong increase of the relativistic electron fluxes at the geosynchronous orbit was observed [*Reeves et al.*, 1998]. The trailing half of the magnetic cloud contained a strong northward IMF and was accompanied by a large density enhancement that strongly compressed the magnetosphere. Because of the significant compression of the magnetosphere, several magnetopause crossings by the geostationary orbit took place. This storm causes also the crash of geostationary satellite Telstar 401 leading to significant financial losses.

Figure 11 shows the Dst and AL indices (Figures 11a and 11b). The hourly averaged Wind data on the plasma and magnetic field are presented in Figures 11c–11e. The time delay (~ 25 min) between the measurements in the Earth's vicinity and on board the Wind spacecraft is taken into account.

The model input parameters were defined by the solar wind density and velocity, by the strength and direction of the interplanetary magnetic field, and by the auroral AL index. Figure 12 presents the time variations of the model input parameters: the tilt angle (Figure 12a) and the magnetic field flux across the magnetotail lobes (Figure 12b). Figure 12c shows b_r, calculated using Burton equation and Dessler-Parker-Skopke equation. Figure 12d shows the distances to the magnetopause subsolar point and to the earthward edge of the tail current sheet.

To investigate the Dst sources during the January 9–12, 1997, event the ground magnetic field was analyzed in terms of the paraboloid model of the magnetosphere A99, which allows us to distinguish the contributions of different large-scale current systems. The paraboloid model calculations are demonstrated in Figure 13 at the left panel. The magnetospheric magnetic field variation is calculated at the geomagnetic equator at each hour of magnetic local time (MLT) and averaged over the equator. Figures 13a–13c (left panel) present the Dst sources Bcf, Br, and Bt and their parts arising owing to the Earth currents. Figure 13d compares the Dst and the calculated magnetic field. A good agreement is obtained for both the relatively quiet and disturbed periods. The calculations in terms of the paraboloid model give an RMS deviation from Dst (δB) of ~ 8.7 nT.

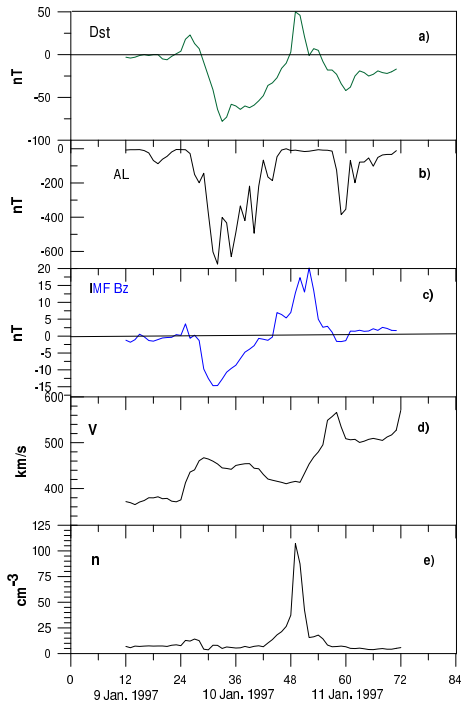

Figure 11: Empirical data used for the calculations of the model input parameters: (a) Dst, (b) AL, (c) IMF B_z component of the solar wind, (d) velocity, and (e) density for January 9–12, 1997.

We can see from the analysis of magnetic storm on January 9–12, 1997, that the magnetospheric dynamics depends on all the magnetospheric magnetic field sources, which appear to be comparable by the order of magnitude. The paraboloid model can be successfully applied, especially in the disturbed periods, when the empirical models are often not valid.

The same magnetic storm was investigated by [Turner et al., 2000] in terms of T96 model. The important feature of the T96 model is (as reported by the author in the T96_01 model's description) its applicability only for 20 nT $> Dst > -100$ nT, 0.5 nPa$< p_{sw} < 10$ nPa, and -10 nT$< Bz_{IMF} < 10$ nT. In the course of the storm under consideration (January 9-12, 1997) the upper value of p_{sw} is significantly beyond the 10 nPa limit. During the most disturbed interval of the magnetic storm under consideration (the first hours of 11 January 1997) T96 model was out of order (see Figure 13, right panel).

The Figure 13 right panel represents calculations made by T96 model in [Turner et al., 2000]. The reason for the residual difference between the calculations presented in [*Alexeev et al.*, 2001] and those made by *Turner et al.* [2000] was investigated in [*Alexeev et al.*, 2001]. This is the tail current inner edge dynamics which are taken into account in the paraboloid model in accordance with the auroral oval expansion due to the substorm activity. In the calculations made by *Turner et al.* [2000] the dynamics of the inner edge of the tail current sheet are neglected.

Thus the discrepancy of the results obtained in [*Alexeev et al.*, 2001] and in that of *Turner et al.* [2000] is explained mainly by the use of different quantitative models and associated with the difference of the tail current parameterization. The quality of a model and its flexibility are defined by the possibility of reflecting the dynamics of the large-scale current systems. The empirical models do not yet allow one to determine correctly the time dependence of each large-scale current system. In the paraboloid model the submodels are used for the calculation of the parameters of the large-scale magnetospheric current systems. These submodels can take into

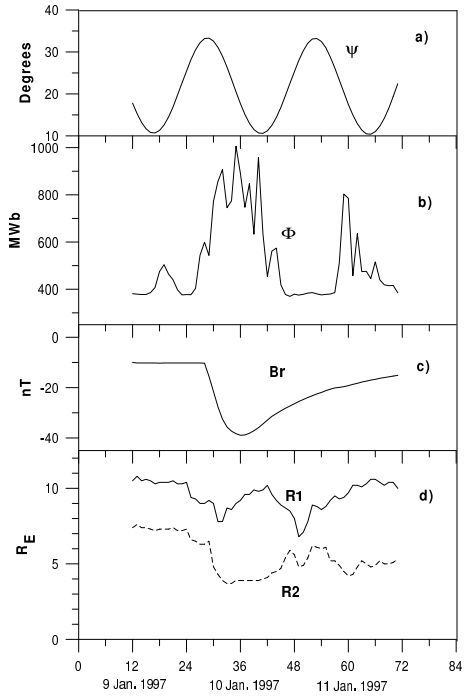

Figure 12: The model input parameters for January 9–11, 1997: (a) the tilt angle, ψ; (b) the magnetic field flux through the magnetotail lobes, Φ_∞; (c) the ring current magnetic field at the Earth's center b_r; and (d) the distances to the magnetopause subsolar point (solid curve), R_1, and to the earthward edge of the magnetotail current sheet (dashed curve), R_2.

account the significant features of various magnetospheric current systems.

The analysis of the magnetic disturbances during the January 9–12, 1997, event shows that in the course of the main phase of the magnetic storm the contribution of the ring current, the currents on the magnetopause, and the currents in the magnetotail are approximately equal to each other by an order of magnitude. Nevertheless, in some periods one of the current systems becomes dominant. For example, an intense Dst positive enhancement (up to +50 nT) in the course of the magnetic storm recovery phase in the first hours on January 11, 1997, is associated with a significant increase of the currents on the magnetopause, while the ring current and the magnetotail current remain at a quiet level. Such analysis can be made only in terms of the modern dynamical models such us paraboloid models, where the different magnetic field sources can be calculated separately. A comparison of the calculated Dst variation with measurements indicates good agreement.

This analysis allows us to investigate the level of applicability of the different kinds of magnetospheric models. The T96 model is not applicable for disturbed periods and does not take into account the time dependence of the important parameters of the magnetospheric current systems. For this reason the most essential part of the magnetotail current system was excluded from the consideration made by *Turner et al.* [2000]. The paraboloid model depends on the parameters of magnetospheric origin and takes into account the movements of the magnetotail in accordance with the level of geomagnetic activity.

To estimate the accuracy of our model calculations of the magnetospheric field at geosynchronous orbit, a comparison with the data obtained on board the geostationary satellites GOES 8 and 9 was performed. For the verification of calculations of the magnetotail current contribution to Dst, the obtained values of the model parameters were used to calculate the auroral oval boundaries, which were compared to the boundaries obtained using the DMSP precipitation

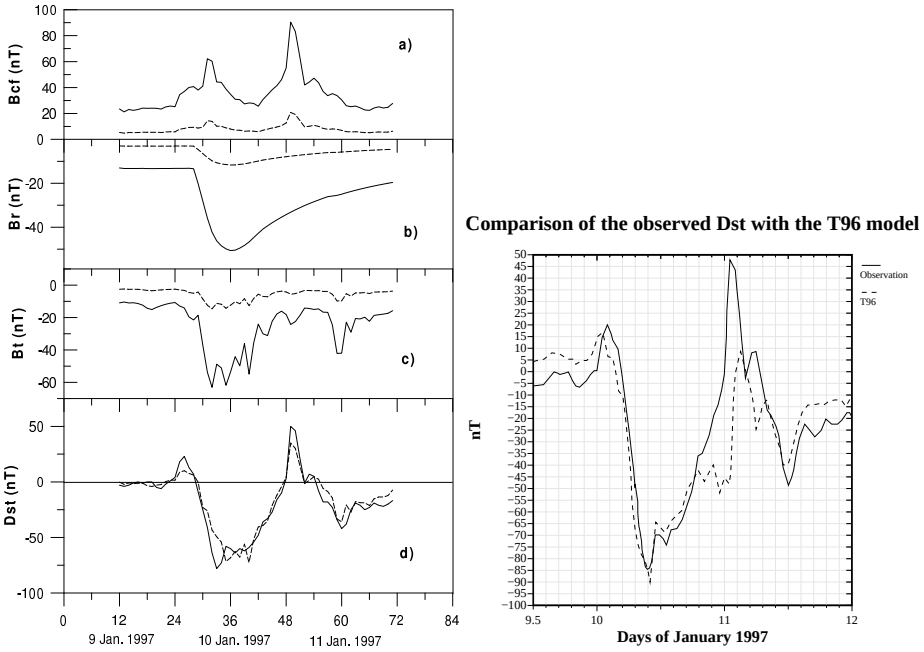

Figure 13: **Left:** (a) Magnetic field of currents on the magnetopause, (b, c) the ring current magnetic field and tail current magnetic field, respectively, at the Earth's surface (solid curves) and the corresponding magnetic field due to currents induced inside the Earth (dashed curves), and (d) Dst (heavy solid curve) and total magnetic field, B_M (dashed curve), calculated at the Earth's surface by A99 in the course of the magnetic storm on January 9–12, 1997. **Right:** Dst (heavy solid curve) and total magnetic field, B_M (dashed curve), calculated at the Earth's surface by T96 in the course of the magnetic storm on January 9–12, 1997 [*Turner et al.*, 2000].

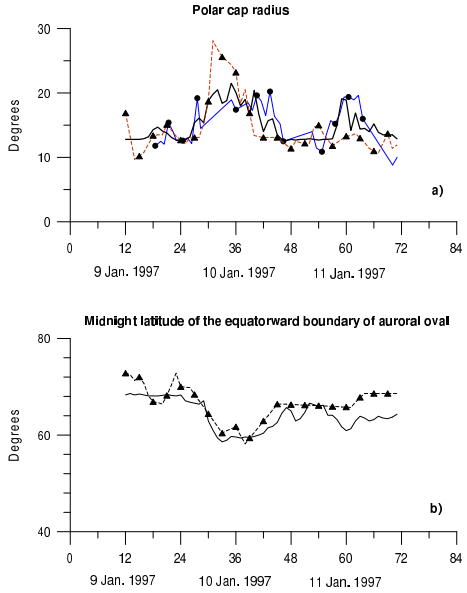

Figure 14: (a) Comparison of the polar cap radius calculated from the magnetic flux value Φ_∞ (solid curve) with radii obtained from the measurements on board DMSP F10-F13 (marked with triangles) and from the Polar Ultraviolet Imager (UVI) images (marked with circles). (b) Comparison of the midnight latitude of the equatorward boundary of the polar oval calculated in terms of paraboloid model (solid curve) and that calculated by the data measurements on board DMSP F10-F13 (marked with triangles).

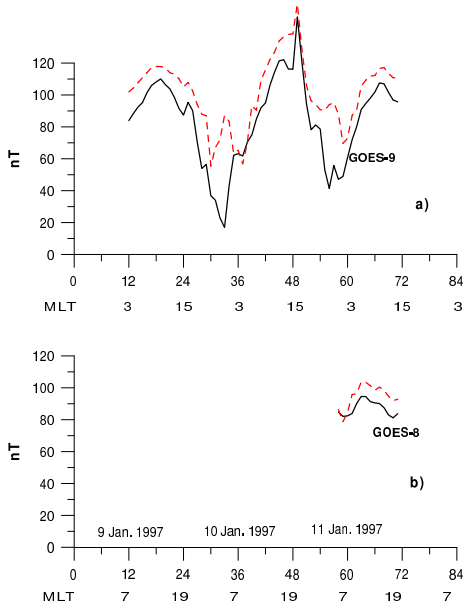

Figure 15: Comparison of the magnetic fields calculated in terms of the paraboloid model and measured during the magnetic storm on January 9–12 , 1997, along the (a) GOES 9 orbit and (b) GOES 8 orbit.

data and the Polar UVI images.

Figure 14a compares the polar cap radius calculated by paraboloid model to the radii obtained from the observations on board DMSP F10-F13 and on board Polar. Figure 14a shows good agreement between the calculations and the experimental data obtained from the independent sources. So, the model estimation of Φ_∞ can be used to identify the polar cap boundaries. Figure 14b compares the midnight latitude of the equatorward boundary of the auroral oval calculated by paraboloid model to those determined using the particle spectra measured on board the DMSP F10-F13 satellites. The obtained agreement with observations confirms our suggestions about Φ_∞ and R_2 made above.

Figure 15 presents the calculations of the magnetic field along the GOES 9 and 8 spacecraft orbits. To take into account the magnetic field of the interterrestrial sources, the International Geomagnetic Reference Field (IGRF95) model was used. The agreement of calculations with the measured magnetic field confirms the initial assumptions of the relative roles of the magnetospheric current systems in the course of magnetic storm.

The usage of the paraboloid model allows one to make an important physical conclusions about the development of the different magnetospheric magnetic field sources during disturbances. We can see that during the main phase of a weak magnetic storm the magnetotail current and the ring current create disturbances of approximately equal intensities. The paraboloid model describes well the magnetic field variations on the Earth's surface and at the geosynchronous orbit during the interaction of a solar wind plasma cloud with the magnetosphere on January 9–12, 1997. The root mean square deviation between the model calculations and the measured field is equal to 8.7 nT. The tail current contribution to the storm maximum disturbance is about -60 nT (for the Dst maximum equal to -78 nT).

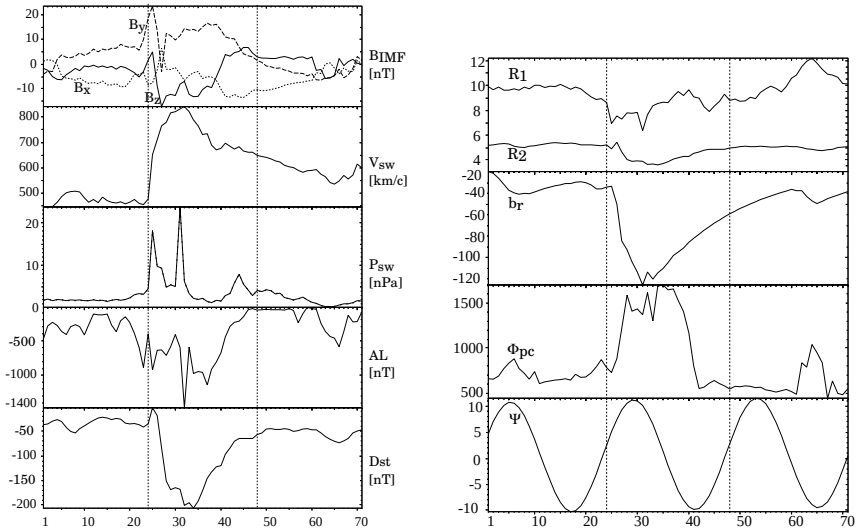

Figure 16: Solar wind data, D_{st}, AL (left panel), and the model parameters $R_1,\ R_2$, both in R_E, b_r [nT], $\Phi_{pc} = \Phi_\infty$ [MWb], and Ψ [$^\circ$] (right).

A3. Nonstationary Case. Magnetic Storm Study on September 24 - 26, 1998

In this sectionwe will demonstrate the advanced technique for magnetic storm investigation which is based on the usage of A01 model and modyfied submodels for calculations of the input parameters.

The magnetic storm on 24-27 September, 1998 will be investigated (see Figure 16). An arrival of a dense cloud of the solar wind plasma at 23:45 on 24 September was accompanied with a northward turning of the IMF, this direction remains for 3 hours. This leads to the interesting phenomena in the Earth's magnetosphere, e.g., to a significant decrease of the polar cap during 30 minutes *Clauer et al.* [2001]. After that the IMF had a strong negative north-south component. Moreover, in 6 hours the second shock wave of the solar wind dense plasma encounters the magnetosphere. At almost the same time a significant substorm activity has been detected (AL index). The both events, however, weakly influenced the dynamics of the D_{st} variation. This behavior of the D_{st} index again attracts attention to the question about dynamics of the magnetospheric current systems and their relative contributions to the magnetic field at the Earth's surface.

In the paraboloid model the magnetic field and D_{st} index are calculated in two stages. Various current systems depend on the concrete parameters unambiguously and a fixed set of these parameters unambiguously defines the magnetic field over the entire magnetosphere.

Calculation of the model parameters in the course of the magnetic storm under consideration made using submodels described below yielded the result presented in right panel of Figure 16. The new submodels other than those used in January 1997 magnetic storm investigation (See A3) were used to provide more accurate calculations. Calculation of the first two parameters are the less contradictory part of this study. The magnetopause subsolar distance, R_1, has been calculated from the pressure balance at the subsolar point. The calculation scheme is based on the iterative procedure.

In order to find the distance to the inner edge of the tail current sheet we have used the results by *Feldstein et al.* [1999] study:

$$R_2 = 1/\cos^2\varphi_n\,, \quad \varphi_n = 64.9^\circ + (|D_{st}|[\mathrm{nT}]/31)^\circ\,. \tag{2}$$

The calculation of the ring current contribution to the D_{st} index is based on the results of *Burton et al.* [1975], *O'Brien and McPheron* [2000] and *Alexeev et al.*, [2001]. Starting from the Dessler-Parker-Sckopke relation between b_r and the ring current particle energy ε_r *Dessler and Parker* [1959] as well as from the injection equation for the dependence of the energy, ε_r, on the time:

$$b_r = -\frac{2}{3}B_0\frac{\varepsilon_r}{\varepsilon_d}, \quad \text{here } \varepsilon_d = \frac{1}{3}B_0 M_E, \quad \text{and } \frac{d\varepsilon_r}{dt} = U - \frac{\varepsilon_r}{\tau}, \tag{3}$$

we received equation for the ring current field:

$$\frac{db_r}{dt} = F(E) - \frac{b_r}{\tau}, \quad \tau\,(hours) = 2.37e^{9.74/(4.78+E_y)}. \tag{4}$$

Here injection function, $F(E)$, is determined by the dawn-dusk solar wind electric field E_y:

$$F(E) = f_{pr}\,(p_{sw})\,f_{ar}\,(AL)\begin{cases} d\cdot(E_y - 0.5) & E_y > 0.5mV/m. \\ 0 & E_y < 0.5mV/m \end{cases} \tag{5}$$

The additional factors $f_{pr}\,(p_{sw})$ and $f_{ar}\,(AL)$ makes it feasible to take into account the influence on the injection of the solar wind dynamic pressure and substorm activity. Large values of the solar wind dynamical pressure increase the effectiveness of injection to the ring current due to increasing of the solar wind plasma transport across magnetopause and into the plasma sheet. AL index shows a fraction of energy flowing directly to the ionosphere. Large values of the AL index or, on the other words, increasing of substorm activity show, from our point of view, that the most part of the energy accumulated in the magnetotail is directly transferred to the ionosphere. That's why the injection to the ring current decreases. These effects are described by factors $f_{pr}\,(p_{sw})$, $f_{ar}\,(AL)$ in Eq. (5).

Using an enormous experience of modelling the magnetic storms and an ideas developed in the present paper we elaborated new submodel describing the dependence of the magnetotail current system on the measurement data. As in the earlier papers (see, e.g., *Alexeev et al.*, [2001]), the magnetic flux in the magnetotail lobes is the key parameter for both the tail current system and the magnetosphere as a whole, being calculated as a sum of two terms:

$$\Phi_\infty\,(t) = \Phi_0\,(t) + \Phi_s\,(t)\,. \tag{6}$$

Here $\Phi_0\,(t)$ is the quiet time value of the magnetic flux, $\Phi_s\,(t)$ is the magnetic flux value associated with the electric field enhancement in the solar wind. To calculate the quiet value, use is made here of our assumption of the basic state of the magnetosphere.

For each value of the solar wind dynamical pressure, the current system parameters for which the energy of the magnetosphere interaction with the solar wind plasma has minimum can be found. At the same time, the characteristic time scale of the current system response to the changes in the interplanetary medium is about one hour. Thus, at the present moment the magnetotail current system tends to realize a state corresponding to the dynamical pressure value of one hour before:

$$\Phi_0\,(t) = 400\cdot\left(p_{sw}\,(t-1)\right)^{1/6.6}. \tag{7}$$

When calculating the dynamical contribution, use was made of the reliable formula *Alexeev et al.* [2001]:

$$\Phi_s\,(t) = b_t\,(t)\,\frac{\pi R_1^2}{2}\sqrt{\frac{2R_1}{R_2}+1}, \tag{8}$$

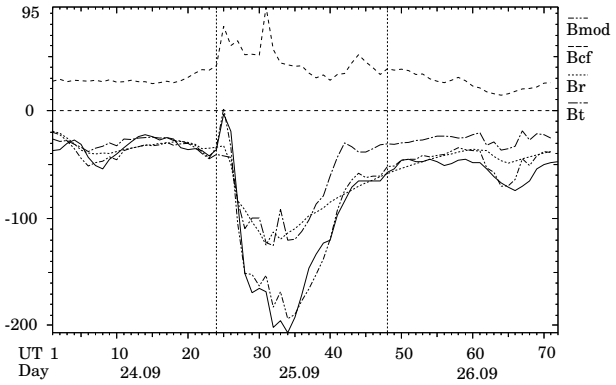

Figure 17: Model magnetic field (dot-dot-dashed curve) vs D_{st} (solid curve). Contributions of magnetopause currents (dashed curve), ring current (dotted curve), and tail current (dot-dashed curve) are demonstrated. One vertical step is 10 nT.

where $b_t(t)$ is the magnetic field of the magnetotail current system near the inner edge of the current sheet. In the earlier study *Alexeev et al.* [2001] this value has been determined using the AL index. This technique is convenient for comparably weak magnetic storms (10-12 January, 1997) in the course of which AL index is a good indicator of both auroral activity and the extent of injection to the ring current. During strong storms and high substorm activity a direct use of the AL index to calculate the contribution of the magnetotail current system is not quite correct, as it is impossible to determine the energy fractions transferred through one or another channel during substorm. In this case only the electric field in the interplanetary medium can be the main measure of energy accumulation in the magnetotail:

$$b_t\left(t\right) = f_{vb}\left(V, B_{imf}, t\right) f_{pb}\left(p_{sw}\right) f_{ab}\left(AL\right) \tag{9}$$

In the above expression the terms f_{ab} and f_{pb} indicate the influence of substorm activity and solar wind dynamical pressure on the tail current. The most essential magnetic field dependence on the electric field in the solar wind is represented by f_{vb} which is determined by the following expression:

$$f_{vb}\left(V, B_{imf}, t\right) = \begin{cases} 0 & b_z \geq 0 \\ \frac{V(t-1)}{300}(b_z\left(t-1\right) - \left|b_y\left(t-1\right)\right| f_{pb}\left(p_{sw}\right)) & b_z < 0 \end{cases} \tag{10}$$

In order to explain this formula we should kept in mind that the current in the current sheet depends mainly on the term $V \cdot b_z$, and one hour delay should be taken into acount. Here one hour was obtained for two reasons. Firstly, this is the minimal time step used when studying magnetic storm and modeling the D_{st} variation. Secondly, an average duration of substorm is also about one hour. Thus, minute time scale would be an overestimation of accuracy.

Figure 17 represents the measured D_{st} - index (see the solid curve) and the magnetic field at the Earth's surface given by the Paraboloid model (see the dot-dot-dashed curve). One can see good agreement of the model calculations with the real D_{st}. The root mean square deviation is about 10 nT. Figure 17 also represents a relative contribution of the large scale magnetospheric current systems to D_{st} (see the figure legend).

A4. Nonstationary Case. Case study for June 25–26, 1998. Comparison with the other models

The cross-comparison of three models based on absolutely different principles (A99, T01, and event oriented G02 [*Ganushkina et al.*, 2002]) was made for the magnetic storm on June 25–26, 1998.

Figure 18 represents the model calculations of the magnetic field along the GOES 8 and 9, Polar and Geotail spacecraft orbits as well as of the Dst in terms of paraboloid model (Figure 18a) and T01 model (Figure 18b) and event-oriented model by [*Ganushkina et al.*, 2002] (Figure 18c). For all the models it shows in GSM coordinates B_x and B_z components of the external magnetic field measured (solid black lines) on GOES 8 (two upper panels), GOES 9 (thrid and fourth panels), on Polar (fifth and sixth panels) and on Geotail (seventh and eighth panels), and calculated using the models (red lines are for Ganushkina's model, blue lines are for A99, and green lines are for T01).

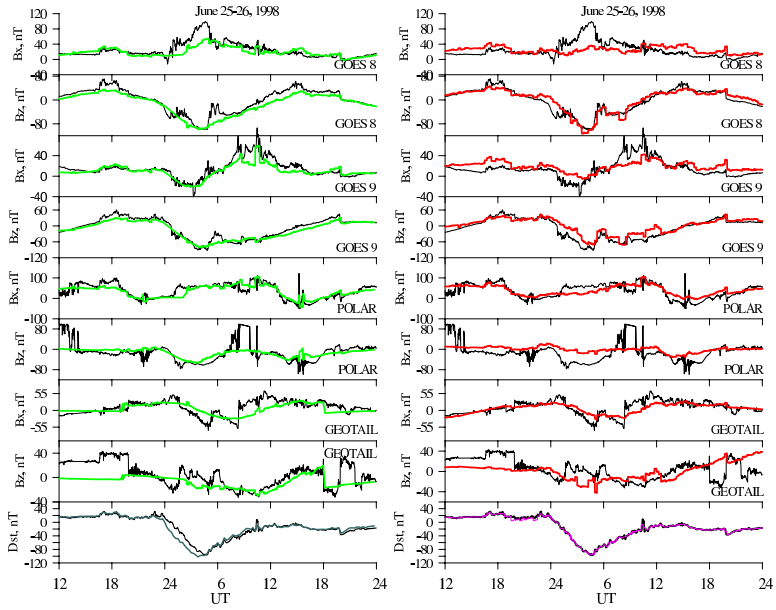

Figure 18: Comparison of calculations in terms of parabolioid model, Ganushkina's model and T01 with calculations on-board GOES 8, 9, Polar and Geotail spacecrafts during magnetic storms on June 25–26, 1998.

We can see that all the models demonstrate the enough good correlation "in general". But every model demonstrate the better accordance in specific comparisons: Ganushkina's model in GOES's B_z component, Polar and Geotail Bx; paraboloid model in GOES's B_x, T02 in GOES's B_z component, both components of Polar.

Acknowledgments. The authors thank N. Tsyganenko NASA GSFC for the magnetosphere magnetic field database and H. Singer, National Geophysical Data Center (NOAA) for the GOES data. Wind data were obtained via on-line CDAWeb service operated by National Space Science Data Center (NASA). The authors thank Tuija Pulkkinen (FMI) for many useful comments and Natasha Ganushkina (FMI) for the presenting results of her model calculations.

References

Alexeev, I. I., Regular magnetic field in the Earth's magnetosphere, *Geomagn. Aeron., Engl. Transl., 18*, 447, 1978.

Alexeev, I. I., E. S. Belenkaya, and C. R. Clauer, A model of region 1 field–aligned currents dependent on ionospheric conductivity and solar wind parameters, *J. Geophys. Res., 105*, 21,119, 2000.

Alexeev, I. I., and S. Y. Bobrovnikov, Tail current sheet dynamics during substorm (in Russian), *Geomagn. Aeron., 37*, 5, 24, 1997.

Alexeev, I. I., and Y. I. Feldstein, Modeling of geomagnetic field during magnetic storms and comparison with observations, *J. Atmos. Sol. Terr. Phys., 63*, 331-340, 2001.

Alexeev I.I., Kalegaev V.V., Belenkaya E.S., Bobrovnikov S.Yu., Feldstein Ya.I., Gromova L.I., Dynamic model of the magnetosphere: Case study for January 9-12, 1997, *J. Geophys. Res.*, **106**, 25,683-25,694, 2001.

Burton, R. K., R. L. McPherron, and C. T. Russell, An empirical relationship between interplanetary conditions and Dst, *J. Geophys. Res.*, **80**, 4204-4213, 1975.

Clauer C. R. Jr., I. I. Alexeev, E. S. Belenkaya, and J. B. Baker, Special features of the September 24-27, 1998 storm during high solar wind dynamic pressure and northward interplanetary magnetic field, *J. Geophys. Res., 106*, 25,695-25,712, 2001.

Dessler, A. J., and E. N. Parker, Hydromagnetic theory of geomagnetic storms, *J. Geophys. Res., 64*, 2239-2252, 1959.

Faierfield et al., A large magnetosphere magnetic field database, *J. Geophys. Res., 99*, 11,319, 1994. Feldstein, Y.I., et al., Dynamics of the auroral elecrtojets and their mapping to the magnetosphere', *Ragiation Measurements, 30*, N 5,1999. 579-587.

Ganushkina, N. Y., Pulkkinen, T. I., Kubyshkina, M. V., Singer, H. J., Russell, C. T., Modeling the ring current magnetic field during storms, *J. Geophys. Res., 107*, SMP 3-1 to SMP 3-13, 2002.

Mead, G.D., and D.H. Faierfield, A quantitative magnetospheric model derived from spacecraft magnetometer data, *J. Geophys. Res., 80*, 523, 1975.

O'Brien, T. P., and R. L. McPherron, An empirical phase space analysis of ring current dynamics: Solar wind control of injection and decay, *J. Geophys. Res., 105*, 7707–7719, 2000.

Olson, W.P., and K.A. Pfitzer, A quantitative model of the magnetospheric magnetic field, *J. Geophys. Res., 79*, 3739, 1974.

Reeves et al., The relativistic electron response at geosynchronous orbit during the January 1997 magnetic storm, *J. Geophys. Res., 103*, 17,559, 1998.

Tsyganenko, N.A., Global quantitative models of the geomagnetic field in the cislunar magnetosphere for different disturbance levels, Planet.Space Sci., 35, 1347-1358, 1987.

Tsyganenko, N.A., A magnetospheric magnetic field model with the warped tail current sheet, Planet. Space Sci., 37, 5-20, 1989.

Tsyganenko, N.A., Modeling the Earth's magnetospheric magnetic field confined within a realistic magnetopause, *J. Geophys. Res., 100*, 5599, 1995.

Turner, N. E., D. N. Baker, T. I. Pulkkinen, and R. L. McPherron, Evaluation of the tail current contribution to Dst, *J. Geophys. Res., 105*, 5431, 2000..